Author response to comments of referee #2: "Spectroscopic evidence for large aspherical β-NAT particles involved in denitrification in the December 2011 Arctic stratosphere"

Atmos. Chem. Phys. Discuss., doi:10.5194/acp-2016-146, in review, 2016
W. Woiwode et al.

We would like to thank referee #2 for his/her time and helpful comments and suggestions to improve the manuscript. In the following, we provide the original referee comments (italic letters) followed by our responses. Text added or modified in the revised manuscript is colored in green.

The authors provide a nice analysis of Fourier transform IR spectroscopic measurements in an Arctic PSC in December 2011. The measurements are analyzed under a variety of radiative transfer situations and with a variety of possible PSC size distributions. The authors convincingly demonstrate the signatures of β-NAT in the data and provide good justification for including the presence of a lower cloud layer and a size distribution with a median radius near 5 µm in the second mode. The paper is well written and should be published. I have three somewhat major comments.

We thank referee #2 for this concise summary and encouraging statement.

1) For those not up on the latest PSC literature. How does β-NAT differ from other NAT? What are the other NAT forms? I assume there is an α-NAT. Is there a γ-NAT?

There are two NAT modifications which are relevant under atmospheric conditions, the thermodynamically stable β-NAT modification and the metastable α-NAT modification. We added the following information:

P2/L4-5: β-NAT is the only nitric acid hydrate known to be thermodynamically stable in condensed state under the conditions of the polar winter stratosphere at temperatures below ~195 K (Hanson and Mauersberger, 1988). The metastable modification α-NAT is another potential PSC constituent at temperatures below ~190 K and transforms irreversibly into β-NAT at higher temperatures (Tizek et al., 2004, and references therein).

2) What is the temperature history of the β-NAT particles sampled? Since the measurement is in December do the presence of these particles provide any information on the possible formation of NAT through heterogeneous nucleation? Did the temperature fall below Tice in the previous days so the nucleation pathways would come through ice? I realize the authors may not wish to pursue this in an already long paper, but it is a natural question which people will be curious about and it may not take much work.

We agree that this aspect, which was investigated by Molleker et al. (2014), is interesting and should be discussed. We added the following:

P4/L33: Molleker et al. (2014) calculated backward trajectories for large particles sampled during the discussed flight and found temperatures close to the frost point ~20 h before the flight. While the model temperatures were too warm for ice nucleation, ice particles might have nucleated during lee-wave-induced cooling above Greenland not resolved by the model. Therefore, it is unclear whether the observed particles have nucleated heterogeneously from ice and/or according to a different mechanism.

3) The discussion of the differences between the condensed hno3 mixing ratio from the various possible size distributions from the different instruments is confusing. Specifically: In section 4, is there an explanation for why the in situ particle size measurements overestimate the condensed phase nitric

acid by about a factor of 2 compared to the MIPAS measurements and compared to what may be realistically expected at these altitudes? Even the MIPAS measurements of ~9 ppbv are not consistent with the HNO3 gas phase deficit shown in Fig. 18, which appears to be about 2-3 ppbv.

We agree that the comparisons of condensed and gas-phase HNO_3 are somewhat difficult to follow. The reason for the higher amounts of condensed HNO_3 derived from the in situ measurements might be an overestimation of the total volume of condensed HNO_3 due to the assumption of spherical particles. Enhancements of gaseous and condensed HNO_3 versus unperturbed conditions are derived from the O_3-HNO_3 correlations in Figure 8. No HNO_3 deficit is found around and below flight altitude. Therefore, the observed excess gas-phase and condensed HNO_3 must have originated from higher altitudes. We clarified these aspects as discussed below.

15.8-9 "The bimodal size distribution A corresponds with 18.2 ppbv gas-phase equivalent HNO3 . . . from the FSSP-100 observations, which corresponds to 18.5 ppbv of gas-phase equivalent HNO3". By gas phase equivalent, I assume the authors mean the gas phase mixing ratio should all the condensed phase hno3 be converted to gas phase? If this is the case please state it more explicitly.

P15/L4: Gas-phase equivalent HNO_3 is calculated for pressure and temperature at flight altitude and corresponds with the volume mixing ratio of gaseous HNO_3 added to the gas-phase if the particles would evaporate instantaneously.

This discussion of condensed hno3 is the most confusing of the paper. What is excess hno3, and condensed excess hno3? Excess to what? I assume excess to some predetermined gas phase mixing ratio determined without particles involved. It is not clear how the gray and black hno3 profiles differ in Fig. 18. From the profiles I guess that the black profile is without particles, but this is not stated.

The authors conclude that the hno3 in the MIPAS determined size distributions, ~8-9 ppbv, is consistent with the gas phase hno3, but would this not mean that all the hno3 is condensed? If I understand Fig. 18 correctly there should be about 2 ppbv hno3 in the particle phase, implying that this is most consistent with CLAMS. The authors should rewrite this section to clarify this discussion.

We thank the referee for pointing out this weakness of the discussion and realize that Figures 8 and 18 require more explanation. Figures 18a to 18c represent the individual gas-phase mixing ratio profiles corresponding with the time interval of the PSC encounter (13:39-14:19 UTC, compare Figs. 2, 6 and 18) and used for the correlation shown in Figure 8. Excess HNO_3 corresponds with HNO_3 exceeding the O_3-HNO_3 correlation under unperturbed conditions (i.e. outside the polar vortex) and results from condensation, sedimentation and evaporation of HNO_3-containing particles (other sources and sinks of HNO_3 and O_3 are neglected).

From the profiles of the individual gases shown in Figure 18 alone, excess HNO_3 (or a HNO_3 deficit) cannot be estimated. Excess (deficit) $HNO_{3(g)}$ is derived by comparing the O_3-HNO_3 correlation during the PSC encounter with the extra-vortex correlation (Figure 8). Excess HNO_3 can be both, gas-phase $HNO_{3(g)}$ and $HNO_{3(s)}$ condensed in the PSC exceeding the extra-vortex correlation (Fig. 8). Since all vortex data points in Figure 18 match or exceed the extra-vortex correlation, any further $HNO_{3(s)}$ condensed in the PSC particles has to be excess HNO_3, too.

The comparison of excess $HNO_{3(g)}$ in the nitrification layer peak with the particle size distributions aims at putting the amounts of condensed $HNO_{3(s)}$ corresponding with the size distributions into a perspective (e.g. assuming that the nitrification layer resulted from instantaneous evaporation of a PSC layer comparable to the PSC layer present around flight altitude).

For clarification, we modified the manuscript as follows:

P7/L19-25: To investigate the accumulated vertical HNO$_3$ redistribution at the locations inside/below the probed PSC, the correlations of the MIPAS-STR HNO$_{3(g)}$ and O$_3$ profiles associated with the PSC encounter (see Fig. 18a and 18c) and profiles outside the polar vortex are shown in Figure 8. O$_3$ is well suited as stratospheric tracer in this case, since the altitude range under consideration is hardly affected by Arctic winter depletion at this early stage of the polar winter. Therefore, deviations of the correlation inside the polar vortex and inside/below the PSC (green data points) from the unperturbed correlation outside the polar vortex (blue data points) indicate excess HNO$_{3(g)}$ or HNO$_{3(g)}$ deficit due to condensation, sedimentation and evaporation of HNO$_3$-containing particles. The comparison of the correlations shows that inside and below the PSC the retrieved HNO$_{3(g)}$ mixing ratios match or exceed the correlation outside the polar vortex. Maximum differences in HNO$_{3(g)}$ of ~5 ppbv are found for O$_3$ mixing ratios around 1.6 to 1.8 ppmv. For the profiles associated with the PSC encounter, this coincides with the altitude range around the nitrification peak at ~16 km (Fig. 6b). Figure 8 furthermore shows that the vortex correlation around flight altitude and inside the PSC (magenta data points) matches or slightly exceeds the extra-vortex correlation extrapolated to higher altitudes (cyan dashed line). This suggests that any HNO$_{3(s)}$ condensed in the PSC particles represents excess HNO$_3$ originating from particle sedimentation from higher altitudes. Denitrified conditions (i.e. data points on the left side of the extra-vortex correlation) are not found in the altitude range covered by the MIPAS-STR observations.

P15/L29-P16/L2: The maximum amount of excess HNO$_{3(g)}$ of ~5 ppbv in the nitrification layer below the flight track (i.e. exceeding the extra-vortex correlation in Fig. 8) is used to put the amounts of condensed HNO$_{3(s)}$ corresponding with the different size distributions into a perspective. HNO$_{3(s)}$ at flight altitude corresponding with the size distributions also represents excess HNO$_3$ originating from higher altitudes, as (i) the O$_3$-HNO$_{3(g)}$ correlation at flight altitude already matches or slightly exceeds the extra-vortex correlation and (ii) the large particle sizes derived from the observations imply significant sedimentation rates and therefore an origin from higher altitudes. Converting the amount of excess HNO$_3$ present at ~16 km in term of molecules per volume to the pressure at the flight altitude of ~18.5 km results in a mixing ratio of ~7.5 ppbv, which is comparable with gas-phase equivalent HNO$_3$ derived from size distributions B, B1 and B2. However, this comparison has to be taken with care, since the excess HNO$_{3(g)}$ in the nitrification layer might have resulted from gradual evaporation of large particles settling into layers with temperatures above T$_{NAT}$ rather than simultaneous evaporation of a certain PSC layer due to raising temperatures. The spatial coincidence of the PSC and the nitrification layer below, the observations of large particles and the fact that temperatures exceed T$_{NAT}$ below the flight path strongly suggest that an ongoing denitrification process was observed and that the nitrification layer below the flight path was associated with the PSC above.
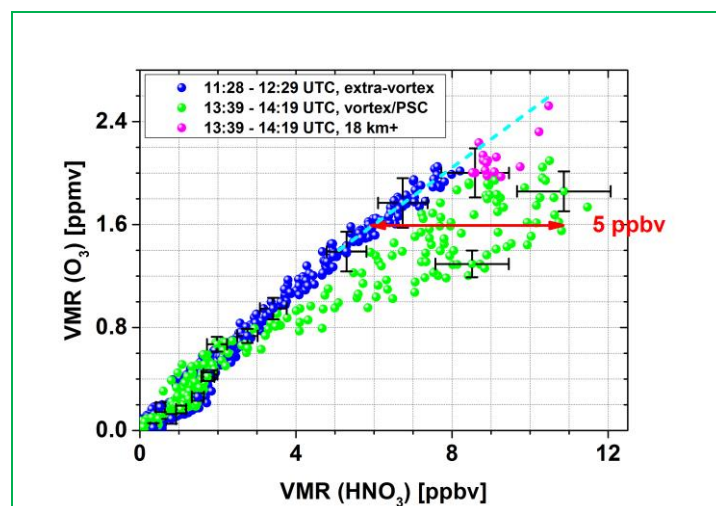
P33/Figure 8:

Figure 8. Correlation of O_3 with $HNO_{3(g)}$ retrieved from the MIPAS-STR observations together with combined random and systematic 1σ-uncertainties of example data points. Blue data points: correlation outside the polar vortex. Green data points: correlation inside the polar vortex and inside/below the observed PSC (data points only where PSC sufficiently transparent for trace gas retrieval, compare Figs. 6b and 17b). Magenta data points are a subset of the vortex data points close to flight altitude ($\geq$18 km) inside the PSC. Cyan dashed line: extrapolation of extra-vortex correlation to higher mixing ratios (i.e. altitudes).

P16/L7-9: in-situ observations. The amount of excess $HNO_{3(g)}$ in the nitrification layer below the flight path is of the same magnitude as $HNO_{3(s)}$ corresponding with size distributions B, B1 and B2.

P17/L2-4: Excess $HNO_{3(g)}$ derived from the MIPAS-STR observations in the nitrification layer below the observed PSC is of the same magnitude as $HNO_{3(s)}$ at flight altitude corresponding with the size distribution supported by the radiative transfer simulations.

17.5-10. Here is a plausible explanation for the discrepancy between the in situ and MIPAS estimates of condensed hno3, but this possibility should be described in section 4 where this discrepancy is discussed.

We agree that it makes sense to discuss this aspect in the section 4 and shifted P17/L5-10 shifted to P16/L5. Together with modifications related to the comments by referee #2 (blue), P16/L4-5 now read as follows:

P16/L4-5: in-situ observations. We mention that Borrmann et al. (2000) investigated the effects of spheroids with AR=0.5 on FSSP observations. Similar to the infrared observations discussed here, the results were close to corresponding Mie calculations. However, the effects of highly aspherical particles on the interpretation of FSSP measurements are uncertain and might explain this discrepancy.

The larger particle sizes derived from the FSSP-100 and CDP measurements using the Mie theory are not necessarily in contradiction with the radiative transfer simulations of the MIPAS-STR observations discussed here when interpreted as maximum dimensions of highly aspherical particles. For example, elongated spheroids with extreme aspect ratios can easily span lengths of several tens of microns while having relatively small individual particle volumes. Evidence of particles with sizes of this magnitude is provided by CIP shadow cast images recorded during the Arctic winter 2009/10 (Molleker et al. 2014).

The CLaMS simulation suggests …

P17/L5-10 replaced by: The discrepancies between the particle size distributions derived from the MIPAS-STR observations and the in situ observations might be due to the fact that spherical particles were assumed in the evaluation of the in situ observations. On the other hand, the particle sizes derived from the in situ observations may be reconciled with the simulations of the MIPAS-STR observations when interpreted as the maximum dimensions of highly aspherical particles.

Minor comments:

Figure 2. Why are there no MIPAS circles above the flight altitude of the Geophysica?

The MIPAS-STR observations are performed in downward-looking mode (limb-mode). Additional upward-viewing measurements are also performed to obtain limited information (mainly column) of atmospheric constituents above the flight path. As a consequence of the measurement geometries, only the downward-looking observations have tangent points along the line-of sight, which are plotted

in Figure 2 (i.e. sampling grid). Upward-viewing measurements could be included into Figure 2 by replacing the vertical axis by vertical viewing angle, which however would not be useful in this context.

The retrieved vertical profiles and vertical cross-sections (Fig. 6, 7, 17 and 18) correspond with the employed retrieval grid (vertical spacing of 0.5 km in the discussed range, see Woiwode et al., 2012). From the combination of the information included in the limb observations and the upward-viewing geometries, some vertically resolved information can be obtained at and slightly above the flight path. However, the vertical resolution decreases rapidly above flight altitude. Therefore, the Figures showing retrieval results (temperature and trace gases) can include data points above the flight altitude.

7.16, "The close agreement of the temperatures measured by MIPAS-STR, the UCSE data and the ECMWF data with calculated TNAT around flight altitude suggests that the observed PSC was composed of β-NAT." Does this correspondence really specifically indicate β-NAT, or just NAT? I have never seen such temperatures specifically target a particular type of NAT. Also what is β-NAT and how does it differ from ??? What is/are the other option(s)? This should be discussed in the introduction.

See above: The existence temperature of β-NAT is higher than for the other atmospheric relevant modification α-NAT and the other potential candidates STS and ice. The potential relevance of α-/β-NAD is addressed in the response to referee #1.

8.11 "In Figure 9a, the particle size distributions derived by Molleker et al. (2014) from the FSSP-100 and CDP observations (black and magenta, respectively) during the PSC encounter are shown." This figure shows observations I think, not a derived size distribution. Please clarify.

We used "derived" to point out that the in situ probes do not directly measure particle size distributions, but particle size distributions are derived from the measured forward scattering signal involving the Mie model or other models. Thereby, the choice of the model, the particle geometry and the particle type has consequences for the resulting size distribution.

9.27 "into the simulated spectra by to the simulated" Fix.

Done.

10.10-32 and Fig. 10. Do we really need to put the reader through all these Mie calculations since the temperatures are clearly too warm for STS and ice? It seems a waste of space to include Figs 10 e)-h) and the discussion of ice and STS, for all the reasons listed at the bottom of page 10. Just state these reasons up front as to why STS and ice are not considered.

We would like to include these plots to show how different refractive indices affect the radiative transfer simulations using the Mie model. In context of the comment by H. Grothe and M. J. Rossi, we furthermore included Mie calculations for α-NAT.

Comment related to most of the Figs 10 -16. A little more effort on the legends in the figure captions would be appreciated. I recognize the space limitations, but the readers do not know what NATcoa means. Why the coa? Nor do the readers know what SP means. I can guess SP10 may mean an aspect ratio of 10 and SP01 an aspect ratio of 0.1, but no directions are provided. Why SP? Use the space to indicate the type of calculation, the type of particle, the aspect ratio, and if possible the median diameter of the second mode

We agree that the legends should be explained in more detail. We mention that information and references for "NATcoa" are given at P8/L2-4 and that the numbers in the legends provide the link to Table 1, which provides all details of the simulations. We modified as follows:

P8/L4: Hereafter, we refer with β-NAT to the "NATcoa" refractive indices by Biermann et al (1998).

P36/L6: 'NATcoa' corresponds with β-NAT and 'Mie' with Mie simulation (AR=1.0).

P37/L5, P38/L5, P41/L6 and P42/L6: 'NATcoa' corresponds with β-NAT, 'TM' with T-matrix simulation and 'SP' with spheroid (numbers indicate AR).

P39/L3: 'NATcoa' corresponds with β-NAT, 'Mie' with Mie simulation, 'TM' with T-matrix simulation and 'SP' with spheroid (numbers indicate AR).

P40/L4: 'NATcoa' corresponds with β-NAT, 'Mie' with Mie simulation, 'TM' with T-matrix simulation and 'SP' with spheroid (numbers indicate AR).

13.13-19. Does the fact that the particles may not be homogeneous, throughout the layer sampled, play a role in diluting/spreading the signal? Are there some minimum number of NAT particles required for the signature?

Horizontally inhomogeneous particle size distributions along the line of sight would modify the observed spectra. However, the spectra measured in different horizontal directions during the PSC encounter (compare Figure 1 with Figures 4a and 4b) show only moderate variations and suggest a relatively homogeneous PSC in horizontal direction.

The minimum particle number densities required for a significant signature depend on (i) the mode radius/radii and width/s of the size distribution, (ii) the vertical thickness of the PSC and (iii) the scattering contribution in the signal as a consequence of the tropospheric cloud scenario and surface temperature and emissivity (see section 3.6). Therefore, the minimum number densities required for a significant signature around 820 cm^{-1} due to the v_2 mode of β-NAT are strongly case-dependent.